

TOPICAL REVIEW

A review of MEMS external-cavity tunable lasers

A Q Liu and X M Zhang

School of Electrical & Electronic Engineering, Nanyang Technological University,
50 Nanyang Avenue, Singapore 639798E-mail: eaqliu@ntu.edu.sg

Received 29 June 2006, in final form 30 October 2006

Published 12 December 2006

Online at stacks.iop.org/JMM/17/R1**Abstract**

The paper reviews the state-of-the-art of miniaturized tunable lasers constructed by microelectromechanical systems (MEMS) technology, covering various topics of laser configurations, theoretical studies and some design issues, with primary focus on the uniqueness of MEMS tunable lasers in comparison to conventional opto-mechanical counterparts. Further studies have also been presented to investigate the tuning range and stability in order to provide a deep understanding of the specialities of MEMS lasers in the sense of physics. The introduction of MEMS has endowed two special features to tunable lasers. One is that MEMS facilitates external cavities at very short ($<100\ \mu\text{m}$) and even extremely short length ($<10\ \mu\text{m}$), leading to unusual tuning behaviors and different design concerns. The other is that the photolithography of the MEMS process makes it possible to fabricate gratings/mirrors in arbitrary profiles, which may inspire the innovation of new laser configurations that can only be realized by MEMS technology. With further work on integration and packaging, MEMS lasers would be able to deliver their merits of small size, fast tuning speed, wide tuning range and IC integration compatibility, and to broaden their applications to many fields.

(Some figures in this article are in colour only in the electronic version)

1. Introduction

With the rapid development of microelectromechanical systems (MEMS) technology, miniaturization of external cavity tunable lasers has recently attracted increasing interest in research and development; some have even led to commercial success [1–3]. MEMS technology makes use of photolithography to fabricate micromechanical structures, which are able to produce complicated movement with fast response, high accuracy and enhanced mechanical stability. Well written reviews on MEMS technology and its applications can be found in [4–8]. MEMS have a natural synergism with external-cavity tunable lasers in various aspects. For example, a semiconductor chip is about several hundred microns long, close to the overall size of a MEMS device (typically 1 mm, including all the functional parts such as

microactuators and suspensions and so on). The wavelength of most tunable lasers is about $0.4\text{--}2\ \mu\text{m}$, on the same scale of the MEMS fine feature. Some types of lasers need a displacement of only about half a wavelength to tune over the whole range [1, 2]; such displacement can be easily obtained using microactuators. In addition, high precision and stable movement of the MEMS structures enable fine tuning of the wavelength with high repeatability. Moreover, the micromechanical structures make it feasible to form very short external cavities ($<100\ \mu\text{m}$), which cannot be realized using the bulky optical components. Most applications such as optical communications and biomedical studies require the tunable lasers to have a wide tuning range ($>40\ \text{nm}$), continuous or stepwise (i.e., discrete) wavelength change, fast speed ($<1\ \text{ms}$), high accuracy/repeatability, high reliability/stability, etc. Some further require lightweight,

easy integration and low cost. The introduction of MEMS to tunable lasers brings in significant improvement in most of these specifications. The small size of MEMS makes the lasers lightweight, portable, easy to form a large array with enhanced mechanical-related properties (e.g., tuning speed, tuning resolution/accuracy and mechanical reliability/stability) in comparison to the conventional lasers. The photolithography of the MEMS process benefits the lasers in terms of accurate positioning/alignment, batch fabrication, easy integration with IC control/monitor circuits, and potentially low cost. More importantly, the ability to construct short cavity makes it promising to obtain a wide tuning range. In some sense, the MEMS technology is revitalizing the tunable lasers.

A MEMS external-cavity tunable laser could be used broadly to describe all the lasers that make use of MEMS structures for the wavelength change. For example, micromachined movable mirrors have been widely used in vertical cavity side-emitting lasers (VCSELs) [9, 10]. Typically the top and bottom mirrors are two oppositely doped distributed Bragg reflectors (DBRs) with a cavity layer (consisting of an active layer and an air gap) in between. The bottom mirror sits on the substrate while the top mirror is suspended by a soft beam, which can be a cantilever beam or a membrane [11, 12]. The air gap can be adjusted by applying an electrostatic potential to attract down the top mirror. As a result, it changes the cavity length and eventually tunes the oscillation wavelength to as far as 30–40 nm [13]. The rapid progress has turned MEMS VCSELs from concepts into commercial success [14, 15]. Due to the very short air gaps, the MEMS VCSELs have no space for optical components and do not need variant optical configurations. From this point of view, the design concern and actual tuning mechanism of the MEMS VCSELs are quite different from those of the edge-emitting tunable lasers. Since the MEMS VCSEL has been extensively reviewed [13, 16–18], this review will not cover this topic. MEMS rotational mirrors have also been employed to select a wavelength from an array of distributed feedback (DFB) lasers [19, 20]. However, this review narrows down to only edge-emitting lasers that make use of the MEMS technology to construct the external cavities with the wavelength selectable lasers excluded.

The terms should also be clarified before further detailed discussion. The change of wavelength in the tunable lasers can be realized in two approaches, one is the continuous shift and the other is mode hopping [21–23]. The form represents the gradual wavelength change if any one of the modes of the laser cavity is monitored. It can happen in either the single longitudinal mode lasers or multiple longitudinal mode lasers when subjected to external feedback. But generally in the single mode lasers, continuous shift over a large range is the primary target while the mode hopping is suppressed. The latter means the peak mode jumps among the cavity modes, leading to an abrupt wavelength change. It happens mostly in multimode lasers. Many works did not tell the difference in claiming the wavelength tuning range [2, 3, 24–32]. For the same amount of continuous shift and mode hopping, the technical difficulties are quite different. For accurate description of the complicated tuning behaviors of the MEMS tunable lasers, the terms of continuous shift and mode

hopping are used to distinguish the two tuning approaches, and correspondingly, shift range and hopping range refer to tuning ranges by each of the approaches. The term wavelength tuning remains unchanged, describing the alteration of wavelength by either of or both the shift and hopping approaches, and the wavelength tuning range refers to the overall range of wavelength change.

Prior to MEMS technology, conventionally macroscopic tunable lasers have been well developed since their advent in 1964 [33]. Details can be found in numerous review articles and textbooks [21, 22, 34–38], which provide a substantial technological database for the MEMS lasers. With the progress of MEMS fabrication capability from wet etching, surface micromachining to deep reactive ion etching (DRIE) [39–41], MEMS tunable lasers have evolved from simple to complicated, from non-continuous tuning to continuous tuning, from a small to a large tuning range, from hybrid integration to single-chip integration, etc [1–3]. Various configurations have been demonstrated [24–32], differing in many aspects of the external cavity such as the external reflectors (i.e., mirrors, etalons, gratings, etc), optical coupling systems, laser chips (normally cleaved or coated) and integration methods (single-chip or hybrid). Some are simple copycat but a miniaturized version of conventional lasers [3], while the others present something new to a certain extent [1, 2, 24–26, 28–31]. In terms of theory, although the MEMS tunable lasers follow the same principles as the conventional bulky counterparts, laser theories and designs should be re-examined since some parameters cannot be simply scaled down. For example, MEMS are able to construct a very short external cavity (e.g. $<10 \mu\text{m}$) [1, 2, 24–26, 31, 32, 42–49], much smaller than the long cavity in bulky tunable lasers (typically $>10 \text{ cm}$). In such a short cavity, the wavelength dependence of the refractive index of the laser gain medium is no longer negligible [29, 50, 51]. The merits of MEMS do not come at no cost. Some technical challenges have arisen, for example, the optical system and the MEMS packaging. The optical quality of micromachined mirrors/gratings is not comparable to the conventional ones. It is also difficult to fabricate three-dimensional (3D) optical systems using the MEMS process without additional assembly. Since MEMS tunable lasers involve movable micromechanical structures, laser chips, optical fibers and even some external optical components (e.g., gratings and ball lenses [3, 52–56]), the packaging and integration would face extreme difficulties in handling, optical alignment and attachment, and may cause mechanical, electrical and thermal stability/reliability problems. Further discussion of MEMS versus conventional laser optics in terms of optical functionalities can be found in [57]. The experimental comparison was shown in [31].

The typical configurations of MEMS tunable lasers will be classified in section 2, with detailed discussions on the merits and constraints. Theoretical analyses of MEMS lasers will be reviewed in section 3, with further studies on the tuning range and tuning stability so as to provide a deep understanding of the uniqueness of MEMS lasers in the sense of physics. Finally, a short discussion will be given on the integration technology of MEMS lasers.

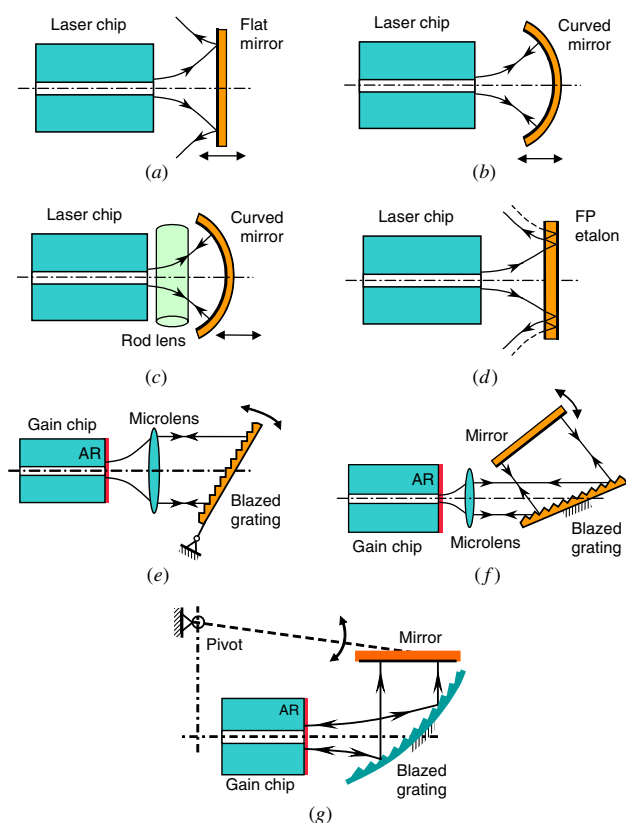


Figure 1. Typical configurations of developed MEMS tunable lasers as classified by external reflectors and micro-optical systems in the external cavities. (a) Lensless scheme, a flat mirror as the external reflector, without any collimation; (b) curved-mirror scheme, a curved mirror to focus in the horizontal direction; (c) 3D-coupling scheme, a curved mirror as the reflector plus a rod lens to focus in the vertical direction; (d) Fabry–Pérot configuration, an etalon as the external reflector; (e) Littrow scheme, a blazed grating in the Littrow configuration; (f) Littman scheme, a blazed grating in the Littman, and (g) non-standard Littman scheme, a blazed grating having variable profile and position of teeth to diffract and collimate the laser beam simultaneously.

2. Laser configurations

Of the many developed MEMS tunable lasers, the tunability is mainly determined by the properties of the external cavity, such as the type of external reflectors, cavity length, feedback strength (i.e., coupling efficiency of the external cavity) and micro-optical system. Below will be discussed the typical laser configurations and their tuning characteristics. It is not intended to give an exhaustive list of the existing MEMS laser configurations, but to merely focus on simple cases so as to present clear physical pictures.

The common configurations of the developed MEMS lasers are illustrated in figure 1, which has seven different schemes but can be roughly categorized into three types, *the mirror configuration*, *the Fabry–Pérot (FP) configuration* and *the grating configuration* as symbolized by the external reflectors. The schemes in figures 1(a)–(c) make use of mirrors as the reflectors; the difference lies in the micro-optical system [1, 2, 24–27, 30, 58–60]. In figure 1(d), a FP etalon is used to form the external cavity [31, 32, 42–49].

In figures 1(e)–(g), gratings play the key roles in forming the resonant cavity and selecting the wavelength [3, 28, 29, 52–55, 61, 62]. In tunable lasers, the reflectors determine the general behavior of the laser tunability. For example, the mirror is a non-dispersive element and presents no filtering effect to the laser beam; if there is no internal wavelength selection mechanism within the laser cavity, the output mode commonly has multiple longitudinal modes, and thus mode hopping and competition can easily happen during the wavelength tuning. In the FP configuration [31, 32, 42–49], the etalon can select a peak mode while suppressing the others; single longitudinal mode is feasible but mode hopping may happen easily. The grating configuration generally employs a blazed grating to select only one mode to oscillate [3, 28, 29, 52–55, 61, 62]. To obtain continuous shift over a large range, a gain chip (i.e., a FP laser chip with one facet antireflection-coated) is used to provide optical gain. Once the reflector type is given, the cavity length and feedback strength will determine more specifically the performance of the ECTL, for example, tuning range, resolution and tuning behavior (discretely, quasi-continuously or continuously, linearly or nonlinearly, stably or chaotically, etc).

2.1. Mirror configuration

It can be seen from figure 1 that the mirror configuration has a simple structure in comparison to the other two. It is thus particularly attractive to research and development. As the emitted laser light in the external cavity should be reflected and then coupled back the internal cavity, it is crucial to have proper design of optical coupling. Based on the micro-optical system, the previous works can be subcategorized into three different schemes as illustrated in figures 1(a)–(c). Figure 1(a) has no optical component for focusing/collimation (named as the *lensless scheme*) [1, 2, 24–26, 31, 58, 59]; figure 1(b) provides focusing in the horizontal direction by simply curving up the shape of the mirror (named as the *curved-mirror scheme*) [27, 60, 63]; and figure 1(c) further improves the focusing/collimation by introducing an additional rod lens (or cylindrical lens, can be implemented by a piece of optical fiber); it thus enables optical coupling in 3D space (named as the *3D-coupling scheme*). The sequence of figures 1(a)–(c) also represents the technical evolution of this type of MEMS laser. The different choices of micro-optical system determine the obtainable length of the external cavity, and affect the tunability of the lasers. More discussions will be presented later in the theoretical analysis part.

2.1.1. Lensless scheme. This is the simplest configuration, without any focusing component in the external cavity. As the laser beam emitted from the end facet has a small spot size and a large divergence angle, the length of the external cavity should be chosen very short so as to maintain an acceptable feedback efficiency. Typically, the emitted Gaussian beam has an elliptical shape with beam waist radii of about 1.0–2.5 μm in the horizontal direction and 0.5–1.8 μm in the vertical direction, while the half divergence angle is commonly 15–40°. Estimations of the coupling efficiency η_{ext} (in terms of optical power, or intensity) with the change of the external cavity length L are plotted in figure 2, with two cases in the

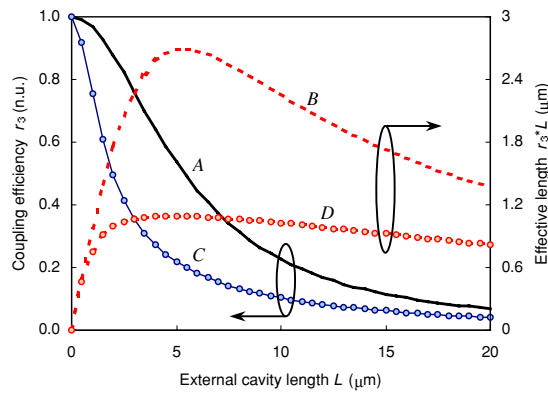


Figure 2. Variations of the coupling efficiency and the effective external cavity length with change of the real external cavity length. The curves labeled *A* and *B* are estimated according to the laser parameters of [2], while *C* and *D* are of [31]. n.u. stands for no unit.

literature as the examples. In one case (curves *A* and *B*), the laser parameters are from [2], in which the wavelength is 1538 nm and the beam radii are 1.75 μm and 1.53 μm . The other case (curves *C* and *D*) is from [31], in which the laser parameters are 980 nm, 2.5 μm and 0.6 μm , respectively. It is assumed in the estimation that the external reflector has 100% reflectivity and perfect alignment to the laser chip. The calculation is based on the mode coupling method developed in [64], which takes into account the divergence and phase change of the Gaussian beam during the propagation. It can be seen in curves *A* and *C* that the coupling efficiency decreases rapidly with longer cavity length. At a 5 μm length, the coupling efficiencies have already dropped to 53% and 21% for the two cases, respectively; at 10 μm , they are 22% and 10%; while at 20 μm , they are as low as only 7% and 4%. Curve *A* is always higher than *C*, implying better coupling for the laser beam that has the larger beam size (relative to wavelength). This explains why the developed MEMS lasers with the lensless scheme always have very short cavity lengths (<20 μm , typically 5–10 μm). Curves *B* and *D* in figure 2 represent the product $\eta_{\text{ext}}*L$, which determines the tuning range and will be elaborated later.

As a MEMS has some difficulty in constructing a high-quality micro-optical system in the external cavity, especially when the structures are fabricated by the deep etching process, the lensless mirror configuration was historically the primary choice of many early MEMS lasers. For example, such configuration was used to detect the resonance of a cantilever beam in 1993 [1]. As shown in the schematic diagram in figure 3(a), a freely suspended cantilever microbeam is sandwiched between two FP laser diodes; all are etched on the same GaAs substrate. One laser diode (LD2) emits an intense pulsed laser to shine on the sidewall of the cantilever. As a result, the induced thermal stress forces the cantilever to vibrate. Maximum vibration amplitude can be obtained when the driving frequency coincides with the resonant frequency of the cantilever. The other laser diode (LD1) emits weak but continuous laser light. It makes use of the other side of the cantilever as the external mirror to form an external cavity, with a separation of only 3 μm . The cantilever vibration alters the cavity length; consequently, the output power of

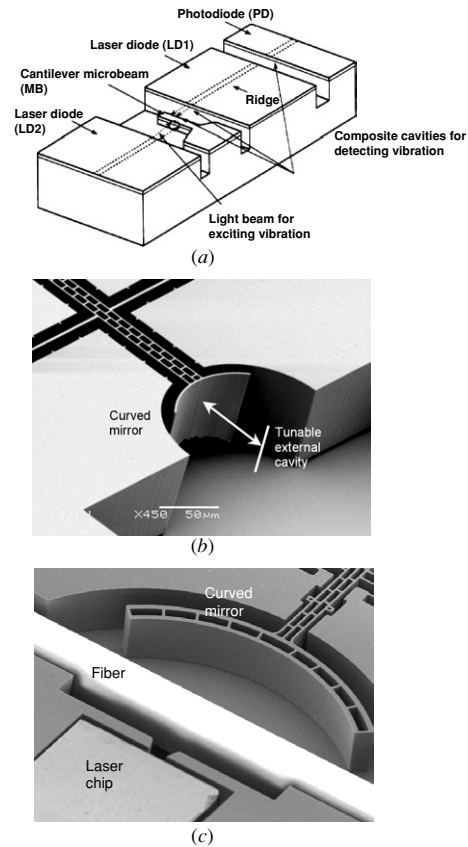


Figure 3. MEMS tunable lasers in the mirror configuration. (a) Lensless scheme [1]; (b) curved mirror scheme [27] and (c) 3D-microsystem scheme [30]. Part (a) reprinted with permission from Ukita *et al* 1993 *Science* **260** 786–9. Copyright 1993 AAAS.

LD1 is varied with the wavelength. In this way, the power change directly represents the vibration amplitude. Although wavelength tuning is not the focus of the work, it had full sense of a real MEMS tunable laser such as the use of external cavity and the change of wavelength. Application of this idea was also proposed to optical disk reading [24]. In 1995 and 1996, the same research group presented further works on wavelength tuning [25, 26]. One utilized an anisotropically etched silicon cantilever beam as the mirror (no metal coating), 10 μm away from a cleaved LD facet [25]. A hopping range of about 3 nm was obtained by a discrete interval of 0.3 nm. Nonlinear movement of the cantilever was produced by a parallel capacitor actuator. In the other work [26], many improvements were made compared with the previous one. The mirror was fabricated by nickel plating, which had higher reflectance. The external cavity was shortened to 5 μm for higher coupling efficiency. Antireflection (AR) coating was applied to the laser facet that faced the nickel mirror, leading to better spectral purity. A comb drive actuator was used to translate the nickel mirror, providing linear and precision displacement and thus accurate wavelength tuning. As a consequence of the improvement, it reported a wavelength change of 20 nm by combination of mode hopping and continuous shift (~ 1 nm range at a 0.01 nm accuracy). A surface-micromachined mirror was also proposed for tunable lasers [65]. A prototype was demonstrated in 2001 [2] in

which an in-plane polysilicon mirror was assembled in the vertical direction and then integrated with a laser chip, with an external cavity length of only $10\ \mu\text{m}$. A wavelength change of $16\ \text{nm}$ was obtained by an alternation of continuous tuning and mode hopping.

Compared with the etched and electroplated mirrors, the surface-micromachined mirror has more flexibility in the mirror size and the optical axis height. However, painstaking manual assembly has to be involved to lift up and fix the mirror to the desired position and angle. Besides, the mirror quality is not ideal due to the etching holes, the residue-stress-induced bending of the mirror and the surface roughness. Generally speaking, these problems make the surface method less attractive. If the mirror quality is the greatest concern, a quick way is to use the polished top surface of a silicon crystalline silicon layer in the silicon-on-insulator (SOI) wafer as the mirror, like in many optical scanners [66, 67]. However, assembly and integration become challenging as the laser chips should be arranged out of the wafer substrate, and it may be difficult to translate the mirror to have a significant change in the laser cavity length. DRIE was also employed to fabricate flat mirrors using the sidewall of etching structures [60]. This fabrication presents some advantages over the other methods. As the etching can be quite deep (typically $75\ \mu\text{m}$), the MEMS structures are robust and stable. It is convenient to pattern the optical components (mirrors and gratings) to complicated profiles. As the mirrors are out of plane after fabrication, no assembly is needed, and the laser chips, optical fibers and other components can be put on the same substrate to facilitate the single-chip integration. There are also some constraints of DRIE. For example, the surface of an etched sidewall is quite rough (typically root mean square roughness $40\ \text{nm}$); the vertical etching has restricted depth, which in turn limits the mirror size in the vertical direction; and the etching can only produce a straight sidewall, that is, no curvature in the vertical direction for laser collimation. However, such constraints can be lifted off. The progress of equipment and process recipes has been improving the surface quality. The introduction of a micro-optical coupling system into the external cavity would be able to converge the laser beam in the vertical direction, solving the problems of mirror size and vertical collimation. For these reasons, the curved-mirror scheme and the 3D-coupling scheme have been proposed for the deep-etched MEMS structures.

2.1.2. Curved-mirror scheme. It is necessary to extend the external cavity length since the longer external cavity bears some technical benefits, such as narrower linewidth, larger tuning range and more space for insertion of other components. For a cavity length $>20\ \text{nm}$, the lensless scheme is not practical. Otherwise, the coupling efficiency will be too low to produce meaningful wavelength tuning. A simple solution is to curve up the mirror surface to converge the reflected laser beam as illustrated in figure 1(b). The beauty of this scheme is that it makes use of a MEMS process to pattern the mirror profile, without need for any further process step and external components. A MEMS laser with such a scheme was presented in 2004 [27]. The mirror had a curvature of $66\ \mu\text{m}$ as shown in figure 3(b). The laser system enabled discrete wavelength tuning by making use of a short

external cavity and weak feedback. A wavelength change of $13.5\ \text{nm}$ was reported by nine steps of mode hopping ($1.69\ \text{nm}$ each step). As the MEMS structure was fabricated by deep etching, the mirror had a straight sidewall and thus no focusing effect in the vertical direction. However, the couple efficiency still can be improved significantly. By estimation, the lensless scheme with an external cavity length of $66\ \mu\text{m}$ has a coupling efficiency of only 0.6% , while the curved-mirror scheme has about 9% [60, 63]. It shows clearly that the curved-mirror enables the extension of the cavity length from several micrometers to several tens of micrometers while maintaining an acceptable coupling efficiency. Due to the focusing effect, the curved-mirror scheme is less tolerable to the position misalignment than the lensless scheme, and the coupling efficiency drops when the mirror is moved way from the best coupling position. Detailed analysis can be found in [63]. It is estimated that the coupling efficiency drops from 9% to 2% in the presence of an angular misalignment of only 1° . And the coupling is reduced to 5% when the external cavity is elongated by $4\ \mu\text{m}$ (causing defocusing). While for the lensless scheme, the coupling efficiency is always kept flat at 0.6% in response to these changes.

2.1.3. 3D-coupling scheme. For ever longer external cavity $>100\ \mu\text{m}$, convergence of a laser beam should be applied in both the horizontal and vertical directions (i.e., in the 3D space). However, at this length the cavity is still not long enough to insert external optical components (such as ball lens, typical diameter $>300\ \mu\text{m}$). A direct approach is to fabricate 3D focus lenses by micromachining and then to integrate with the MEMS lasers. Tremendous effort has been put into developing Fresnel zone plates [68] or thermal reflowed photoresist microlenses [69–73]. However, it remains a challenge to fabricate 3D microlenses directly on the sidewall of a deep-etched structure. Most of the current methods fabricate the microlenses on the surface of a substrate or holder, and then lift up and fix them to the vertical direction [68–70]. An alternative approach to form 3D focus is to use two cylindrical lenses, one in the horizontal direction and the other in the vertical direction [74]. The cylindrical lenses are fabricated by SU-8 with a height of $200\ \mu\text{m}$. The lenses are taken from the substrate, rotated by 90° and then pressed into the hosts (trenches in the SU-8 layer) in the desired position. Although it reported good results of collimation and focusing, it is difficult to incorporate into the MEMS tunable lasers due to assembly difficulty and accuracy. Another solution is to introduce a rod lens (i.e., cylindrical lens) into the curved-mirror scheme as shown in figure 1(c). The rod lens provides the collimation/focus of a laser beam in the vertical direction, and thus ensures high coupling efficiency even at a longer cavity length. The 3D-coupling scheme was presented in a recent work as shown in figure 3(c) [30]. The curved mirror was deep etched on a SOI wafer. The coupling efficiency measured 46.5% for a cavity length of $220\ \mu\text{m}$ and dropped to 40% after displacing the mirror by $4\ \mu\text{m}$, showing much higher coupling efficiency and larger tolerance to mirror displacement. One of the interesting parts of this work is that a piece of single mode optical fiber is used as the rod lens. It brings in many advantages since the fiber is easily available and convenient for handling, aligning

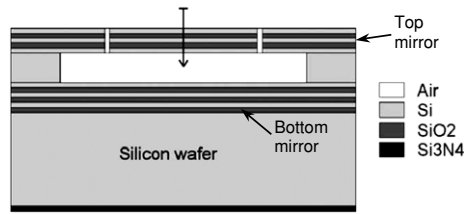


Figure 4. MEMS tunable lasers in the Fabry–Pérot configuration, which use Fabry–Pérot etalon as the external reflectors [32]. Reprinted with permission from Heikkinen *et al* 2004 *IEEE Photon. Technol. Lett.* **16** 1164–6. Copyright 2004 IEEE.

and packaging. The diameter of the fiber can be tailored by the HF etching (etching rate $3.5 \mu\text{m min}^{-1}$ for Corning SMF-28 in 49% HF solution). The fiber core has negligible influence on the focus/collimation effect since the refractive index difference is only 0.36% and the core is only $8.2 \mu\text{m}$ in diameter in comparison to $125 \mu\text{m}$ of the fiber cladding [75, 76]. By carefully designing the curved mirror and the fiber rod lens, the external cavity can be extended to a longer distance. In this way, the MEMS tunable laser may have a full range of cavity length, from an extremely short cavity ($<10 \mu\text{m}$), very short cavity ($<100 \mu\text{m}$), short cavity ($<1 \text{mm}$) to a long cavity, without the need for conventional bulky optical components (lenses, reflectors, etc).

2.2. Fabry–Pérot configuration

This configuration employs a FP etalon (as illustrated in figure 1(d)) for wavelength selection, which improves the spectral purity of the laser output, such as the single longitudinal mode and high side mode suppression ratio (SMSR). The concept was proposed and realized by serial works [42–49]; extensive analyses and experimental studies can be found in [31]. As shown in the schematic diagram in figure 4 [32, 47], the etalon consists of a movable top mirror and a fixed bottom mirror, which is formed by many alternative quarter-wave layers of polysilicon and silicon dioxide. The reflectance of the etalon is 97%. By applying voltage between the mirrors, the top mirror is moved toward the bottom and the spectral transmission band is tuned to a shorter wavelength as given by the relationship $m\lambda = 2l$ (m is the interference mode number and should be an integer, $m = 3$ in this work; λ is the central wavelength of the FP pass band and l is the air space between the two mirrors). The central wavelength is 1540nm and the external cavity length is chosen to be $75 \mu\text{m}$. By carefully adjusting the cavity length through piezoelectric stage and the etalon space, both multimode and single mode tunings were demonstrated with a range of 13nm and improved spectral quality (narrower linewidth and higher SMSR). This configuration has three FP cavities, the etalon, the internal laser cavity and the external cavity. Limited by the space for a laser chip, the movable top mirror of the etalon is located inbetween the laser facet and the fixed bottom mirror. With the movement of the top mirror, the external cavity length is changed with the etalon length simultaneously. Careful choice of the initial condition and good match of the cavities are critical for stable wavelength tuning [31]. Otherwise, the tuning can be complicated and unstable.

2.3. Grating configuration

Many applications require the lasers to be tuned continuously while maintaining the single longitudinal mode. According to the arrangement of the gratings, the developed MEMS lasers can be classified into three schemes: the *Littrow scheme*, *Littman scheme* and *non-standard grating scheme* as shown in figures 1(e)–(g), respectively. The Littrow and Littman schemes are simply the downsized version of the conventional lasers [3, 28, 55, 61], in which gratings have straight baseline and require the incident beam well collimated. In these two schemes, lenses have to be used for laser collimation and focusing. As the common materials of a MEMS structure layer have high optical refractive index, the use of lenses invites quite high Fresnel reflection losses in the interfaces with the air. For example, single crystalline silicon has the refractive index $n = 3.482$ at 1550nm , each Si/air interface loses the optical power by $R = (n - 1)^2 / (n + 1)^2 = 30.6\%$. After a roundtrip in the external cavity, only 23.1% of the laser power is left. To tackle this problem, it is desirable to use a reflector rather than a lens to collimate the laser beam. Moving the idea a step forward, it is possible to combine the reflector and the grating to form a non-standard grating, which has curved baseline and serves the purpose of collimation and diffraction simultaneously as shown in figure 1(c) [62]. As the MEMS process makes use of photolithography for patterning, non-standard gratings can be easily fabricated. This is one of the special merits that MEMS endows to tunable lasers.

2.3.1. Littrow scheme. In this scheme, the laser is collimated to and diffracted by the blazed grating at the same angle as shown in figure 1(e). It is a single-pass diffraction, i.e., the light is diffracted only once in the external cavity. The wavelength tuning is realized by rotating the grating about a remote pivot [28, 29, 53–55]. Compared with the other two schemes, the Littrow scheme has high coupling efficiency and simple tuning structure, and thus has attracted many research interests. For example, a deep-etched grating was integrated with a ball lens to form a Littrow laser [54], which reportedly obtained a wavelength tuning range of 120nm . Micromechanical tuning flexures were contrived to obtain a remote pivot for the rotation of grating [53, 55, 56]. A single-chip integrated laser was presented by fabricating the microlens, blazed grating and tuning mechanical structures on the same chip as shown in figure 5(a) [28, 29]. After integration of the MEMS parts with the gain chip and optical fiber, the device has dimensions of only $2.0 \text{mm} \times 1.5 \text{mm} \times 0.6 \text{mm}$ and can be continuously tuned over a range of 30.3nm . Although the obtained output power (typically 1mW) is quite weak in comparison to the conventional counterparts, mainly due to the low diffraction efficiency of the MEMS gratings and the poor thermal conductivity of the silicon substrate, the developed lasers have demonstrated the merits of MEMS such as fast tuning speed, small size and single-chip integration.

Like the conventional lasers, MEMS Littrow lasers suffer from a fundamental limitation that the wavelength tuning range cannot be very large (typically $<30 \text{nm}$) if the pivot for the grating rotation is fixed [29, 77–79]. This is due to the mismatching of wavelength selection mechanisms. In the Littrow scheme as shown in figure 1(e), two mechanisms

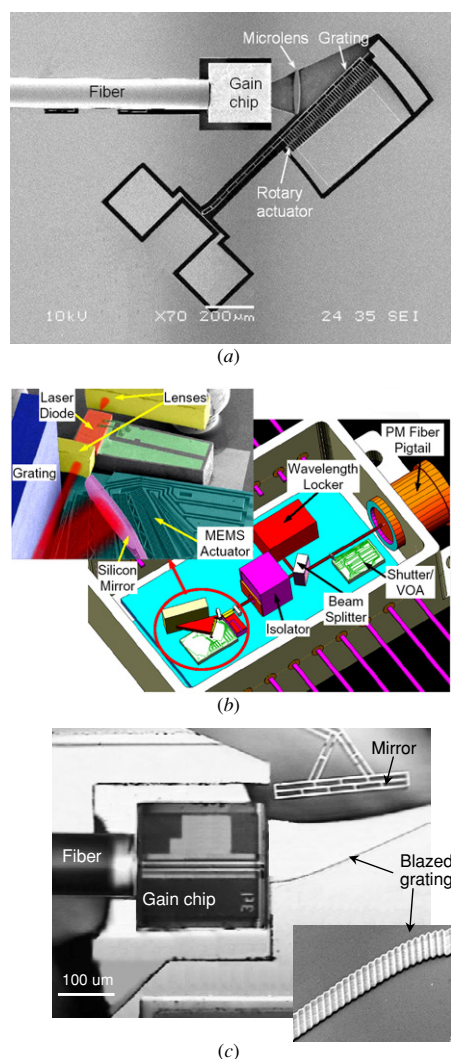


Figure 5. MEMS tunable lasers in the grating configuration, which uses blazed gratings as the external reflectors. (a) Single-chip integrated tunable laser in the Littrow scheme [28, 29]; (b) hybridly integrated tunable laser in the Littman scheme [3, 52] and (c) tunable laser in the non-standard grating scheme, which makes use of a patterned grating for focus and diffraction of a laser beam simultaneously [62]. Part (a) reprinted with permission from Zhang *et al* 2005 *IEEE J. Quantum Electron.* **41** 187–97. Copyright 2005 IEEE.

contribute to the wavelength selection. One is the diffractive grating while the other is the FP resonant cavity formed by the uncoated laser facet and the grating [22, 23, 29]. To obtain continuous tuning, the wavelengths selected by the grating and the FP should always match each other when the grating is rotated about a remote pivot. However, such a match cannot be maintained for long when the pivot position is fixed. The grating selects the wavelength by the Bragg condition, in which the wavelength is varied by a relationship of the sine curve with the rotation angle of the grating. In contrast, the FP cavity length is changed by the tangential curve, while the wavelength is linear to the cavity length. That is to say, one is the sine curve while the other is tangential; thus the mismatch would accumulate with the higher rotation angle (corresponding to the increase of wavelength tuning) and eventually break the continuous tuning. This limitation is not due to MEMS but the

geometric arrangement of the gain chip relative to the grating. To overcome this problem, one method is to move the pivot position with the rotation of grating. MEMS is able to realize this function, but needs complicated mechanical structures and may encounter the mechanical stability problem. A preferred method is to implement the Littman scheme into the MEMS lasers.

2.3.2. Littman scheme. This scheme has one more mirror in comparison to the Littrow scheme as shown in figure 1(f) [3, 52, 61]. The collimated beam is diffracted by the grating, reflected by the mirror and then diffracted again before being coupled into the gain chip. It is double-pass diffraction, i.e., the laser beam is diffracted twice in a roundtrip of the external cavity. Unlike the rotational grating in the Littrow scheme, the grating of the Littman scheme is fixed while the mirror is rotated about a remote pivot for wavelength tuning. The geometric arrangement of this scheme does not impose any constraint to the tuning range [35–37]. Here the FP cavity length is arranged to change by a sine curve (no more tangential curve) with the rotation angle, exactly the same with the sine relationship in the blazed grating. That is, the two wavelength selection mechanisms can be identical at any angle. Therefore, a large tuning range can be easily obtained with a fixed pivot, making it very attractive for industrial products. The Littman MEMS tunable lasers were demonstrated in 2001 and were later commercialized successfully [3, 52]. Figure 5(b) shows the device architecture with a close-up of the MEMS structures in the inset. A silicon mirror is mounted on a specially designed comb drive actuator [52, 80–82], whose rotation by $\pm 1.4^\circ$ produces a continuous wavelength tuning over 40 nm. In another work, a Littman laser was demonstrated by constructing a virtual pivot using MEMS flexures; it reported a tuning range of 65 nm by an angular rotation of 3.6° . However, hybrid integration has to be used in the reported works since the optical lenses, gratings, mirrors are external components. The Littman scheme requires grazing incidence to the grating, which helps to cover more grating teeth at a given laser beam size and thus obtains a narrower linewidth, but results in low diffraction efficiency, especially when the grating is fabricated by micromachining.

2.3.3. Non-standard grating scheme. A recent work demonstrated the use of variable grating profile to realize the collimation and diffraction of a laser beam simultaneously [62]. Such grating is different from the standard blazed gratings that have straight or concave profiles [73], and is thus called non-standard grating. The concept is as shown in figure 1(g); detailed expressions of the position and profile of the grating teeth were presented in [62]. The basic idea is that by gradually varying the position and angle of each grating tooth, the optical paths that pass through the adjacent grating teeth has a fixed phase difference of $m2\pi$ (m is integer, the order of diffraction) when they reach a certain plane (where the mirror sits). The rotation of the mirror introduces an extra phase difference and thus tunes the wavelength. Similar ideas can be found in the concave gratings [83] and replicated holographic gratings [84–86] that sit the grating teeth on a spherical or curved surface so as to focus and diffract the laser beam simultaneously. Some recent works shared this idea in

patterning the planar waveguide to form lenses and gratings for tunable lasers, though the tuning is not based on MEMS but on the refractive index change by the injected electrical current [87, 88].

The MEMS device is shown in figure 5(c). The tuning structure is fabricated by deep etching on a SOI wafer, and is then integrated with the gain chip and optical fiber onto a single chip, with a footprint of only $3 \text{ mm} \times 2.5 \text{ mm}$. The grating teeth have varying position and profile, but share the same period of $3.32 \mu\text{m}$ if projected to the equiphase plane (i.e., the mirror surface). It reported a tuning range of 9.2 nm. This particular design does not need a lens for collimation, and thus circumvents the losses induced by the micromachined lenses or the extra assembly of external lenses. In addition, it avoids the use of grazing incidence to the grating, which causes low diffraction efficiency in the Littman scheme. Although the tuning range is quite limited in the reported work [62], it demonstrates the potential of MEMS in enabling new laser tuning configurations, which is not practical for conventional lasers due to the fabrication difficulty of gratings.

3. Theoretical development

MEMS tunable lasers follow the same general physical principles as the conventional ones, which have been extensively analyzed and reviewed in [38, 89, 90]. However, MEMS tunable lasers may exhibit certain uniqueness in the aspects of tuning behaviors and design considerations since the MEMS technology provides different working conditions such as short cavity length and high coupling efficiency. For instance, the extremely short cavity length ($< 10 \mu\text{m}$) of the MEMS lasers makes it feasible to obtain a large hopping range in the mirror configuration [63], which cannot be realized by the conventional lasers with a long cavity length ($> 1 \text{ cm}$). For this reason, efforts have been made to revisit the laser theories and to adapt them to the MEMS cases [29, 59]. This section will try to summarize the previous theoretical works and further develop them for studying the tuning range and tuning stability.

3.1. Tuning range and stability of mirror configuration

The short cavity length and the high coupling efficiency are the dominant factors that distinguish the MEMS lasers from the conventional ones in terms of tuning behaviors such as the continuous tuning range, stability of tuning and mode hopping range. Generally, single mode lasers focus on continuous tuning, while multimode lasers target at discrete tuning (i.e., controllable mode hopping with well suppressed continuous shift).

3.1.1. Continuous shift. In the presence of external reflection, the output wavelength of the laser will be shifted with the change of the external cavity length. Under weak feedback strength, such wavelength shift $\Delta\lambda$ was derived in [38, 89], as given by

$$\Delta\lambda = \frac{\lambda_0^2}{2\pi L} \frac{C \sin[2\pi\tau_L\nu_0 + \arctan(\alpha)]}{1 + C \cos[2\pi\tau_L\nu_0 + \arctan(\alpha)]} \quad (1)$$

where λ_0 and ν_0 are the central wavelength and frequency, respectively; L is the external cavity length; τ_L is the roundtrip

delay of the external cavity given by $\tau_L = 2L/c_0$ (c_0 denotes the light velocity in vacuum); α is the equivalent linewidth enhancement factor given by $\alpha = \alpha_0/\Gamma_0$ (α_0 is the linewidth enhancement factor of the gain medium and Γ_0 is the optical confinement factor); and $C = (L/\mu_0 d_0)\xi\sqrt{1+\alpha^2}$ represents the external feedback strength, where μ_0 is the refractive index of the laser gain medium, d_0 is the length of the internal laser cavity, $\xi = r_3(1-r_2^2)/r_2$ is the relative reflectance of the external mirror, and r_3 and r_2 are the amplitude reflectance of the external mirror and the laser facet facing the external mirror, respectively. Here r_3 is not directly the reflectance of the mirror but the coupling efficiency of the external cavity, with mirror reflectance and coupling losses (due to the mirror misalignment and the spreading of a laser beam) taken into consideration. A correction is made to include the influence of the optical confinement factor Γ_0 , which has a small value (typically 0.05–0.1 for ridge-waveguide multiple-quantum-well InGaAsP/InP lasers) and significant influence to the tuning range but was overlooked in some previous analyses [38, 59, 89].

Equation (1) describes the basic relationship between the continuous shift and the change of the external cavity length. It should be highlighted that the derivation of equation (1) is based on one explicit assumption $\xi \ll 1$ (called the weak feedback condition) and two implicit assumptions: one is that the laser is single longitudinal mode (called the single mode condition) and the other is $\tau_L\Delta\nu \ll 1$ (called the small tuning condition), where $\Delta\nu = c_0\Delta\lambda/\lambda_0^2$ is the shift of central frequency. These three conditions define the applicability of the analysis. In MEMS lasers, they should be re-examined. The small tuning condition is equivalent $\Delta\lambda \ll \lambda_0^2/2L$, i.e., the tuning range is limited by the free spectral range (FSR) of the external cavity. It implies that the short cavity allows a larger tuning range. Under the single mode condition, the laser tuning is continuous with the increase of the external cavity, at a period of half a wavelength. However, when this condition is broken, the tuning behavior becomes complicated. This explains why the experiments observe a combination of continuous tuning and mode hopping when multiple longitudinal lasers are used [2, 25, 26, 31]. The weak feedback condition $\xi \ll 1$ requires $r_3 \ll r_2$, that is, the feedback from the external mirror is relatively weak in comparison to the laser facet reflection. This is why the model is called the weak feedback model. An extension of the model was presented to cover both the weak and medium feedback regions based on the assumption that $r_2 r_3 \ll 1$ [59]. This model is more suitable for some MEMS lasers, especially those having extremely short cavity and high feedback coupling efficiency. For instance, it can be read from figure 23 of [31] that $r_3 = 0.3$ – 0.4 when the external cavity is 5 – $10 \mu\text{m}$. If the laser facets are normally cleaved, then it has $\xi \approx 0.45$, which is no longer a weak feedback. With the same parameters, $r_2 r_3 \approx 0.18$, the condition of $r_2 r_3 \ll 1$ is held roughly. In this case, the extended feedback model has to be used.

One of most important parameters of the tunable laser is the shift range $\Delta\lambda_r$. Based on equation (1), it can be further derived that

$$\Delta\lambda_r = \frac{\lambda_0^2}{2\pi} \frac{A_0}{\sqrt{\frac{1}{r_3^2} - A_0^2 L^2}} \quad (2)$$

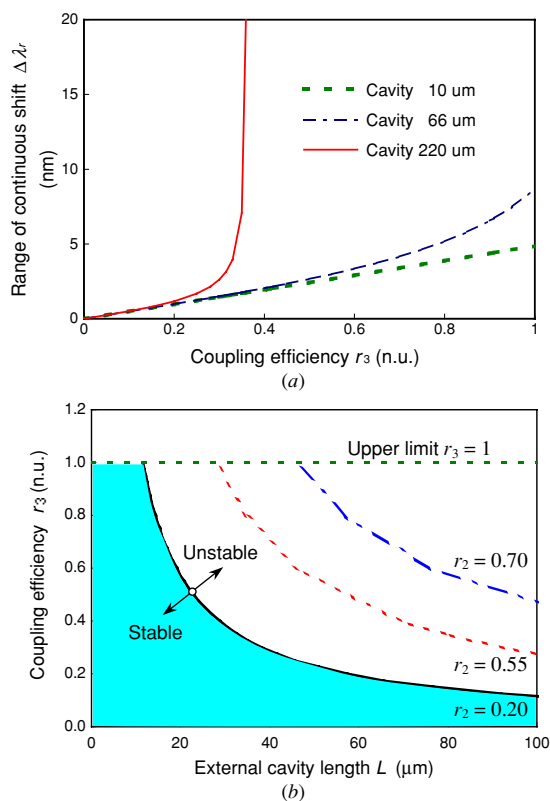


Figure 6. Influence of coupling efficiency and external cavity length on wavelength tuning range. (a) Wavelength tuning range versus external coupling efficiency for different cavity lengths [30]; (b) stable region of laser operation at different reflectance of the internal laser facet. n.u. stands for no unit.

where $A_0 = (1 - r_2^2)\sqrt{1 + \alpha^2}/r_2\mu_0d_0$ is a variable determined by the parameters of the internal laser cavity; its value increases with smaller r_2 and shorter internal cavity length. Equation (2) directly links the shift range to the external mirror reflectance and the external cavity length. The relationship is illustrated in figure 6(a) [30]. For a given cavity length, higher coupling efficiency results in a larger shift range. In figure 6(a), the shift range for the cavity of 66 μm is increased gradually to 8.7 μm when r_3 rises from 0 to 1, while at a given coupling efficiency, the longer external cavity length produces more continuous shift. For example, if the coupling efficiency is fixed at $r_3 = 0.8$, the shift range is estimated to be 5.2 nm for external cavity lengths of 10 nm, in comparison to the 3.9 nm shift of the 66 nm cavity.

3.1.2. Stable region and effective external cavity length. It can be seen from figure 6(a) that for the cavity length of 220 nm, the wavelength tuning shoots up at $r_3 \approx 0.36$, which corresponds to the stability problem (or coherence collapse) of the tuning lasers. It was observed experimentally that the laser runs through five different regimes successively when the external coupling increases from very weak to very strong in comparison to the laser facet reflectance [91]. Coherence collapse [92–94] occurs in the fourth regime (i.e., not very strong feedback) with the appearance of drastic broadening of linewidth and loss of coherence of light beam. The condition

of stable operation can be easily derived from equation (2) as given by

$$r_3L < 1/A_0 \quad (3)$$

plus one more limit $r_3 \leq 1$. Examples of the stable operation regions are shown in figure 6(b) for different levels of laser facet reflectance. The shadowed area is the stable region for the condition $r_2 = 0.20$. The parameters are taken as $\alpha = 3$, $\Gamma_0 = 0.1$, $\mu_0 = 3.482$, $d_0 = 300 \mu\text{m}$. At $r_2 = 0.20$, $1/A_0 = 11.5 \mu\text{m}$. The area below $r_3 = 1$ and $r_3L = 11.5$ defines the stable region. Outside this region, the laser operation becomes unstable. In other words, at a given level of r_3 the external cavity length cannot be too long. For example, in the case of perfect coupling (i.e., $r_3 = 1$), the external cavity length should be shorter than 11.5 μm . When r_2 is increased to 0.55 and 0.70, the stable region is widened as illustrated in figure 6(b). That is to say, longer L is allowed with the increase of r_2 if r_3 is kept constant. This is due to that the increase of r_2 causes a decrease of laser facet transmittance and thus less laser light can be coupled back into the laser internal cavity.

The above analysis provides another angle to understand the operation of external cavity lasers. For example, in a lensless external cavity where r_3 changes with L , the product of r_3L is more directly related to the shift range than the individual variables r_3 and L . Therefore r_3L is named as the effective length of the external cavity. It was demonstrated by numerical simulation in [31] that the lensless scheme runs through three successive tuning regions with the increase of the external cavity length: the reduced tuning region in which the cavity length is close to 0 and has small wavelength tuning; the nonlinear tuning region that has largest wavelength tuning; and the linear tuning region that has the wavelength tuning limited by the FSR of the external cavity. The observation of the three regions was explained by treating the external cavity as an introduced loss curve to move over the gain curve [31]. The concept of effective length can provide a more straightforward explanation. From curves B and D of figure 2, the effective length has roughly three different parts: it is always small at the beginning, and then increases gradually to the peak, followed by a decrease at larger L . As the longer effective length results in the larger wavelength tuning range, the three parts of the effective length curve directly correspond to the reduced, the nonlinear and the linear tuning regions, respectively, as observed in [31]. The concept of effective length also provides a guideline for the design of the lensless scheme; the external cavity length should be chosen near to the peak of the effective length.

3.1.3. Hopping range of multimode lasers. Multi-longitudinal-mode lasers may exhibit complicated behavior of wavelength change in response to an external feedback since the existence of many oscillation modes could easily cause the peak mode to hop among some of the modes in addition to the continuous shift. It is commonly observed in the experiment that the wavelength of peak mode experiences an alternation of continuous shift and mode hopping when the external cavity is lengthened or shortened continuously, at a period of half a wavelength [2, 25, 26, 31, 58]. If the amount of continuous shift is negligible in comparison to the FSR of the laser cavity, the output wavelength is dominated by mode

hopping, i.e., discretely tuning as demonstrated in [27, 63]. According to equation (3), the discrete tuning requires weak coupling efficiency and short cavity length, exactly opposite to those conditions for single mode lasers that target at large continuous shift. In order to determine the maximum hopping steps, the external cavity can be approximately treated as a FP filter superimposed on the longitudinal modes of the internal laser cavity. Therefore, the hopping range λ_h and the maximum hopping steps M are limited by the FSR of the external cavity:

$$\Delta\lambda_h \leq \lambda_0^2/2L \quad (4a)$$

$$M \leq \mu_0 d_0/2L. \quad (4b)$$

For example, in the MEMS laser of [27] $L = 66 \mu\text{m}$ and $d_0 = 210 \mu\text{m}$, it has $M \leq 11$ according to equation (4b). The experiment actually observed nine stable hopping steps plus two unstable steps [27, 63]. For comparison, assuming a conventional laser with $L = 10 \text{ cm}$, it has $M \leq 0.01$; actually no mode hopping is allowed. It can be seen from the examples that the MEMS tunable lasers can realize discretely tuning using simply the mirror configuration, while the conventional long cavity lasers cannot. This is another special merit of the MEMS tunable lasers.

3.2. Optimization of the continuous tuning range in grating configuration

The short cavity length influences the design of MEMS lasers in the grating configuration through the change of the gain medium refractive index in the internal laser cavity. Detailed discussion and analysis can be found in [29, 63]; here we try to give a simple physical picture of this issue. Commonly the internal laser cavity is treated as fixed in the laser design. However, the effective refractive index μ_e of the gain medium actually varies with the tuning of the external cavity by two mechanisms. One is due to the wavelength dependence of the InGaAsP refractive index [50, 51]; in the region near $1.55 \mu\text{m}$, μ_e decreases with higher λ at a rate of $\Delta\mu_e \approx -0.334\Delta\lambda/\lambda_0$ [29, 63]. The other is that the external coupling efficiency r_3 is actually reduced with the rotation of grating due to the change of diffraction efficiency, which in turn affects the carrier density of the gain medium and finally causes a reduction of the refractive index. The relation is estimated to be $\Delta\mu_e \approx -0.092\Delta\lambda/\lambda_0$ in the study of [29, 63]. By estimation, the cavity length will be shortened by about $2.0 \mu\text{m}$ relative to its nominal value when the wavelength is tuned by 30 nm . Such discrepancy might be negligible for long cavity lasers, but would significantly affect the achievable continuous tuning range in the short cavity lasers. According to the experiments in [28, 29], the tuning range is 30.3 nm when the refractive index change is considered, in contrast to only 5.9 nm when not included.

4. Discussions

The design of MEMS tunable lasers should compromise between various parameters once the target is given, while to prototype the lasers, different integration approaches have been practiced. Brief discussions are presented here on the cavity length and integration approach.

4.1. Short cavity versus long cavity

The choice of cavity length is dependent on the goal of tunable lasers and the parameters of a laser chip. If continuous tuning is the primary target, the laser facet that forms the external cavity should be AR coated. In this case, the wavelength tuning range is determined by $\Delta\lambda_r/\lambda_0 = \Delta L/L_0$, where ΔL and L_0 are the cavity length change and the initial cavity length, respectively. It can be seen that a small L_0 leads to a large $\Delta\lambda_r$, i.e., the short external cavity is preferable for the large tuning range. If discrete tuning is the focus, the short cavity is also preferable according to equations (4a) and (4b). Under one condition that the reflectivity of the laser facet in the external cavity is larger than or at least comparable to the external coupling efficiency, the long cavity is important to obtain large continuous shift as depicted by equation (2).

4.2. Hybrid integration versus single-chip integration

The core part of a MEMS external-cavity tunable laser typically consists of at least three separated components: a gain medium for optical amplification, an external reflector (mirror or grating) plus a microactuator for wavelength tuning and an optical coupling system in between. Two approaches have been followed to integrate all these components to form a standalone device: hybrid integration and single-chip integration [95]. The former uses the MEMS structure to replace the bulky tuning mechanics but keeps the other parts unchanged, while the latter aims at fabricating most of the tunable laser components using the MEMS process and then integrating the whole laser onto a single chip. Hybrid integration is often the first of many alternative choices, especially in commercial products; it allows a smooth shift from the conventional tunable lasers to the MEMS ones and thus bears less risk. A successful example of hybrid integration was the MEMS continuously tunable lasers that were commercialized [3, 52]. Such hybridization well improves the tuning speed and mechanical stability, but the size cannot be reduced since the bulky optical components remain. Single-chip integration makes full use of the MEMS technology and incorporates many advantages of MEMS into the tunable lasers. The microfabricated reflectors and their micromechanical actuators are very light, yielding better tuning properties; the integration further reduces the overall dimension. The on-chip fabrication of optical components makes optical packaging/integration unnecessary, resulting in high yield and low cost; moreover, it facilitates more functional subsystems that consist of several MEMS components such as the optical add/drop multiplexers and injection-locked lasers [96, 97]. Therefore, the single-chip integration represents the trend of further development.

5. Conclusions

Application of MEMS technology to construct the external cavity of a tunable laser represents a natural trend to downscale bulky devices, and introduces significant improvement in many specifications such as tuning speed, wavelength tuning range and mechanical stability. More importantly, the MEMS tunable laser stands out from conventional ones by facilitating a very short external cavity and arbitrary grating/mirror

profile, which cause different wavelength tuning behaviors and design concerns, and enables new laser configurations. The developed MEMS lasers have been demonstrated in various designs. According to the type of external reflector, the micro-optical system and the arrangement of gratings, they can be roughly summarized into three configurations and can be further categorized into seven schemes, each has its own wavelength tuning characteristics. The theoretical works on MEMS lasers have adapted the ready theories under the condition of very short external cavity, and have analyzed the topics of continuous shift, mode hopping tuning stability and change of gain medium refractive index. MEMS tunable lasers are still young compared with conventional lasers. One of the main challenges is the difficulty of packaging as the MEMS structures, laser chips, optical fibers and control circuits have to be integrated. More work should be done before the MEMS lasers are able to provide a single-chip solution for real applications.

Acknowledgments

The authors gratefully acknowledge the support by the Agency for Science, Technology and Research (A*STAR) of Singapore under grant no 042 108 0097. Zhang would like to thank the Singapore Millennium Foundation (SMF) for the Research Fellowship. Special thanks go to Dr Jing Li, Mr Yu Aibin and Ms Hong Cai for their helpful discussions and providing useful information for this study.

References

- [1] Ukita H, Uenishi Y and Tanaka H 1993 A photomicrodynamic system with a mechanical resonator monolithically integrated with laser diodes on gallium arsenide *Science* **260** 786–9
- [2] Liu A Q, Zhang X M, Murukeshan V M and Lam Y L 2001 A novel device level micromachined tunable laser using polysilicon 3D mirror *IEEE Photon. Technol. Lett.* **13** 427–9
- [3] Berger J D and Anthon D 2003 Tunable MEMS devices for optical networks *Opt. Photon. News* **14** 42–62
- [4] Judy J W 2001 Microelectromechanical systems (MEMS): fabrication, design and applications *Smart Mater. Struct.* **10** 1115–34
- [5] Walker J S 2000 The future of MEMS in telecommunications networks *J. Micromech. Microeng.* **10** R1–7
- [6] Lin L Y and Goldstein E L 2002 Opportunities and challenges for MEMS in lightwave communications *IEEE J. Sel. Top. Quantum Electron.* **8** 163–72
- [7] Trimmer W 1996 *Micromechanics and MEMS: Classic and Seminal Papers to 1990* (New York: IEEE)
- [8] Fujita H 1998 Microactuators and micromachines *Proc. IEEE* **86** 1721–32
- [9] Chen Q, Cole G D, Björölin E S, Kimura T, Wu S, Wang C S, MacDonald N C and Bowers J E 2004 First demonstration of a MEMS tunable vertical-cavity SOA *IEEE Photon. Technol. Lett.* **16** 1438–40
- [10] Cole G D, Björölin E S, Chen Q, Chan C-Y, Wu S, Wang C S, MacDonald N C and Bowers J E 2005 MEMS-tunable vertical-cavity SOAs *IEEE J. Quantum Electron.* **41** 390–407
- [11] Li Y M, Yuen W, Li G S and Chang-Hasnain C J 1998 Top-emitting micromechanical VCSEL with a 31.6-nm tuning range *IEEE Photon. Technol. Lett.* **10** 18–20
- [12] Larson M C, Massengale A R and Harris J S 1996 Continuously tunable micromachined vertical cavity surface emitting laser with 18 nm wavelength range *IEEE Electron. Lett.* **32** 330–2
- [13] Chang-Hasnain C J 2000 Tunable VCSEL *IEEE J. Sel. Top. Quantum Electron.* **6** 978–87
- [14] Vakhshoori D, Tayebati P, Lu C-C, Azimi M, Wang P, Zhou J-H and Canoglu E 1999 2 mW CW single mode operation of a tunable 1550 nm vertical cavity surface emitting laser with 50 nm tuning range *IEEE Electron. Lett.* **35** 900–1
- [15] Vail E C, Li G S, Yuen W and Chang-Hasnain C J 1996 High performance micromechanical tunable vertical cavity surface-emitting lasers *IEEE Electron. Lett.* **32** 1888–9
- [16] Chang-Hasnain C J 2000 Widely tunable VCSEL using MEMS technology *Proc. 13th LEOS Annual Meeting (Rio Grande, Puerto Rico, 13–17 November 2000)* pp 54–5
- [17] Syms R R A and Moore D F 2002 Optical MEMS for telecoms *Mater. Today* **5** 26–35
- [18] Pezeshki B 2001 New approaches to laser tuning *Opt. Photon. News* **12** 34–8
- [19] Pezeshki B *et al* 2002 20-mw widely tunable laser module using DFB array and MEMS selection *IEEE Photon. Technol. Lett.* **14** 1457–9
- [20] Souhaite G, Blondeau R, Delepine S, Pellegrini O, Vassilakis E, Stellmacher M, Graindorge P and Martin P 2001 16 channels, switchable external cavity-based multi-wavelength laser for DWDM applications *Proc. ECOC'01, 27th European Conf. on Optical Communication (Amsterdam, The Netherlands, 30 September–4 October 2001)* vol 2 pp 196–7
- [21] Amann M-C and Buus J 1998 *Tunable Laser Diodes* (Boston: Artech House)
- [22] Duarte F J 1995 *Tunable Lasers Handbook* (London: Academic)
- [23] Ye C 2004 *Tunable External Cavity Diode Lasers* (Singapore: World Scientific)
- [24] Ukita H, Uenishi Y and Katagiri Y 1994 Applications of an extremely short strong-feedback configuration of an external-cavity laser diode system fabricated with GaAs-based integration technology *Appl. Opt.* **33** 5557–63
- [25] Uenishi Y, Tsugai M and Mehregany M 1995 Hybrid-integrated laser-diode micro-external mirror fabricated by (110) silicon micromachining *IEEE Electron. Lett.* **31** 965–6
- [26] Uenishi Y, Honma K and Nagaoka S 1996 Tunable laser diode using a nickel micromachined external mirror *IEEE Electron. Lett.* **32** 1207–8
- [27] Zhang X M, Liu A Q, Tang D Y and Lu C 2004 Discrete wavelength tunable laser using microelectromechanical systems technology *Appl. Phys. Lett.* **84** 329–31
- [28] Liu A Q, Zhang X M, Tang D Y and Lu C 2004 Tunable laser using micromachined grating with continuous wavelength tuning *Appl. Phys. Lett.* **85** 3684–6
- [29] Zhang X M, Liu A Q, Lu C and Tang D Y 2005 Continuous wavelength tuning in micromachined Littrow external-cavity lasers *IEEE J. Quantum Electron.* **41** 187–97
- [30] Zhang X M, Cai H, Lu C, Chen C K and Liu A Q 2006 Design and experiment of 3-dimensional micro-optical system for MEMS tunable lasers *Proc. MEMS 2006, 19th IEEE Int. Conf. Micro Electro Mechanical Systems (Istanbul, Turkey, 22–26 January 2006)* pp 830–3
- [31] Aikio J K 2004 Extremely short external cavity (ESEC) laser devices *VTT publication 529, ESPOO 2004* <http://www.vtt.fi>
- [32] Heikkinen V, Aikio J K, Alojoki T, Hiltunen J, Mattila A-J, Ollila J and Karioja P 2004 Single-mode tuning of a 1540-nm diode laser using a Fabry-Pérot interferometer *IEEE Photon. Technol. Lett.* **16** 1164–6
- [33] Crowe J W and Craig R M Jr 1964 GaAs laser linewidth measurement by heterodyne detection *App. Phys. Lett.* **5** 72–4

- [34] Coldren L A, Fish G A, Akulova Y, Barton J S, Johansson L and Coldren C W 2004 Tunable semiconductor lasers: a tutorial *IEEE J. Lightwave Technol.* **22** 193–202
- [35] Littman M G and Metcalf H J 1978 Spectrally narrow pulsed dye laser without beam expander *Appl. Opt.* **17** 2224–7
- [36] Littman M G 1978 Single-mode operation of grazing-incidence pulsed dye laser *Opt. Lett.* **3** 138–40
- [37] Liu K and Littman M G 1981 Novel geometry for single-mode scanning of tunable lasers *Opt. Lett.* **6** 117–8
- [38] Petermann K 1988 *Laser Diode Modulation and Noise* (London: Kluwer)
- [39] Li J, Liu A Q and Zhang Q X 2006 Tolerance analysis for comb-drive actuator using DRIE fabrication *Sensors Actuators A* **125** 494–503
- [40] Li J, Zhang Q X and Liu A Q 2003 Advanced fiber optical switches using deep RIE (DRIE) fabrication *Sensors Actuators A* **102** 286–95
- [41] Li J, Zhang Q X, Liu A Q, Goh W L and Ahn J 2003 Technique for preventing stiction and notching effect on silicon-on-insulator microstructure *J. Vac. Sci. Technol. B* **21** 2530–9
- [42] Aikio J K and Karioja P 1999 Wavelength tuning of a laser diode by using a micromechanical Fabry-Pérot interferometer *IEEE Photon. Technol. Lett.* **11** 1220–2
- [43] Aikio J K, Sidorin, Blomberg M and Karioja P 1999 Wavelength tunable hybrid laser diode realized by using an electrostatically tuned silicon micromachined Fabry-Pérot interferometer *Proc. SPIE 3625, part of the SPIE Conf. on Physics and Simulation of Optoelectronics Devices VII (San Jose, CA, 25–29 January 1999)* pp 588–97
- [44] Aikio J K, Kataja K J and Howe D G 2001 Extremely short external cavity lasers: direct semiconductor laser readout modeling by using finite difference time domain calculations *Proc. SPIE 4595, Photonics Systems and Applications (Singapore, 28–30 November 2001)* pp 163–73
- [45] Aikio J K, Kataja K J, Alajoki T, Karioja P and Howe D G 2002 Extremely short external cavity lasers: the use of wavelength tuning effects in near field sensing *Proc. SPIE* **4640** 158–69
- [46] Sidorin Y, Blomberg M and Karioja P 1999 Demonstration of a tunable hybrid laser diode using an electrostatically tunable silicon micromachined Fabry-Pérot interferometer device *IEEE Photon. Technol. Lett.* **11** 18–20
- [47] Blomberg M, Orpana M and Lehto A 1996 Electrically tunable Fabry-Pérot interferometer produced by surface micromechanical techniques for use in optical material analysis *US Patent* 5 561 523
- [48] Sidorin Y and Howe D 1998 Some characteristics of an extremely-shortexternal-cavity laser diode realized by butt coupling a Fabry-Pérot laser diode to a single-mode optical fiber *Appl. Opt.* **37** 3256–63
- [49] Sidorin Y, Karioja P and Blomberg M 1999 Novel tunable laser diode arrangement with a micromachined silicon filter: feasibility *Opt. Commun.* **164** 121–7
- [50] Burkhand H, Dinges H W and Kuphal E 1982 Optical properties of $\text{In}_{1-x}\text{Ga}_x\text{As}_y\text{P}_{1-y}$, InP, GaAs, and GaP determined by ellipsometry *J. Appl. Phys.* **53** 655–62
- [51] Broberg B and Lindgren S 1984 Refractive index of $\text{In}_{1-x}\text{Ga}_x\text{As}_y\text{P}_{1-y}$ layers and InP in the transparent wavelength region *J. Appl. Phys.* **55** 3376–81
- [52] Anthon D, Brenger J D, Drake J, Dutta S, Fennema A, Grade J D, Hrinya S, Ilkov F, Jerman H, King D, Lee H, Tselikov A and Yasumura K 2002 External cavity diode lasers tuned with silicon MEMS *Proc. OFC 2002, Opt. Fiber Commun. Conf. Exhibit (Anaheim, CA, 17–22 March 2002)* pp 97–8
- [53] Syms R R A and Lohmann A 2002 Tuning mechanism for a MEMS external cavity laser *Proc. Optical MEMS 2002, IEEE/LEOS Int. Conf. Optical MEMS (Lugano, Switzerland, 20–23 August 2002)* pp 183–4
- [54] Lohmann A and Syms R R A 2003 External cavity laser with a vertically etched silicon blazed grating *IEEE Photon. Technol. Lett.* **15** 120–2
- [55] Syms R R A and Lohmann A 2003 MOEMS tuning element for a Littrow external cavity laser *IEEE J. Microelectromech. Syst.* **12** 921–8
- [56] Syms R R A, Lohmann A and Huang W 2005 MOEMS laser tuning element with an indirect drive *Proc. Optical MEMS 2005, IEEE/LEOS Int. Conf. Optical MEMS (Oulu, Finland, 1–4 August 2005)* pp 11–2
- [57] Kim S, Barbastathis G and Tuller H L 2004 MEMS for optical functionality *J. Electroceram.* **12** 133–44
- [58] Zhang X M, Liu A Q, Murukeshan V M and Chollet F 2002 Integrated micromachined tunable lasers for all optical network (AON) applications *Sensors Actuators A* **97–98** 54–60
- [59] Liu A Q, Zhang X M, Murukeshan V M, Lu C and Cheng T H 2002 Micromachined wavelength tunable laser with an extended feedback model *IEEE J. Sel. Top. Quantum Electron.* **8** 73–9
- [60] Liu A Q, Zhang X M, Li J and Lu C 2003 Single-/multi-mode tunable lasers using MEMS mirror and grating *Sensors Actuators A* **108** 49–54
- [61] Huang W, Syms R R A, Stagg J and Lohmann A 2004 Precision MEMS flexure mount for a Littman tunable external cavity laser *IEEE Proc. Sci. Meas. Technol.* **151** 67–75
- [62] Zhang X M, Cai H, Liu A Q, Hao J Z, Tang D Y and Lu C 2005 MEMS Littman tunable laser using curve-shaped blazed grating *Proc. Transducers '05, 13th Int. Conf. on Solid State Sens. Actuat. Microsystems (Seoul, Korea, 5–9 June 2005)* pp 804–7
- [63] Zhang X M 2006 Theory and experiment of MEMS tunable lasers *PhD Thesis* School of Electrical and Electronic, Nanyang Technological University
- [64] Yuan S and Riza N A 1999 General formula for coupling-loss characterization of single-mode fiber collimators by use of gradient-index rod lenses *Appl. Opt.* **38** 3214–22
- [65] Kiang M-H, Solgaard O, Muller R S and Lau K Y 1996 Silicon-micromachined micromirrors with integrated high-precision actuators for external-cavity semiconductor lasers *IEEE Photon. Technol. Lett.* **8** 95–7
- [66] Piyawattanametha W, Patterson P R, Hah D, Toshiyoshi H and Wu M C 2005 Surface- and bulk-micromachined two-dimensional scanner driven by angular vertical comb actuators *IEEE J. Microelectromech. Syst.* **14** 1329–38
- [67] Tsou C, Lin W T, Fan C C and Chou B C S 2005 A novel self-aligned vertical electrostatic combdrives actuator for scanning micromirrors *J. Micromech. Microeng.* **15** 855–60
- [68] Lee S S, Lin L Y, Pister K S J, Wu M C, Lee H C and Grodzinski P 1995 Passively aligned hybrid integration of 8×1 micromachined micro-Fresnel lens arrays and 8×1 vertical-cavity surface-emitting laser arrays for free-space optical interconnect *IEEE Photon. Technol. Lett.* **7** 1031–3
- [69] King C R, Lin L Y and Wu M C 1996 Out-of-plane refractive microlens fabricated by surface micromachining *IEEE Photon. Technol. Lett.* **8** 1349–51
- [70] Fletcher D A, Crozier K B, Guarini K W, Minne S C, Kino G S, Quate C F and Goodson K E 2001 Microfabricated silicon solid immersion lens *IEEE J. Microelectromech. Syst.* **10** 450–9
- [71] Wu M-H and Whitesides G M 2002 Fabrication of two-dimensional arrays of microlenses and their applications in photolithography *J. Micromech. Microeng.* **12** 747–58
- [72] Pan L-W, Shen X and Lin L W 2004 Microplastic lens array fabricated by a hot intrusion process *IEEE J. Microelectromech. Syst.* **13** 1063–71
- [73] Jay T R and Stern M B 1994 Preshaping photoresist for refractive microlens fabrication *Opt. Eng.* **33** 3552–5
- [74] Hsieh J, Weng C-J, Lin H-H, Yin H-L, Hu Y C, Chou H-Y, Lai C-F and Fang W 2003 The study on SU-8 micro cylindrical lens for laser induced fluorescence application *Proc. Optical MEMS 2003, IEEE/LEOS Int. Conf. Optical MEMS (HI, USA, 18–21 August 2003)* pp 65–6

- [75] Corning® SMF-28™ 2001 optical fiber product information, Corning Inc. 1–4
- [76] Maeda M, Ikushima I, Nagano K, Tanaka M, Nakashima H and Itoh R 1977 Hybrid laser-to-fiber coupler with a cylindrical lens *Appl. Opt.* **16** 1966–70
- [77] Soffer B H and McFarland B B 1967 Continuously tunable, narrow-band organic dye lasers *Appl. Phys. Lett.* **10** 266–7
- [78] McNicholl P and Metcalf H J 1985 Synchronous cavity mode and feedback wavelength scanning in dye laser oscillator with gratings *Appl. Opt.* **24** 2757–61
- [79] de Labachellerie M and Passadat G 1993 Mode-hop suppression of Littrow grating-tuned lasers *Appl. Opt.* **32** 269–74
- [80] Grade J D, Jerman J H and Kenny T W 2003 Design of large deflection electrostatic actuators *IEEE J. Microelectromech. Syst.* **12** 35–43
- [81] Jerman J H and Grade J D 2002 Balanced microdevice and rotary electrostatic microactuator use *US Patent* 6 469 415
- [82] Jerman J H and Grade J D 2005 Balanced microdevice *US Patent* 6 903 486
- [83] Hutley M C 1982 *Diffraction Gratings* (London: Academic)
- [84] Cohen A L 1989 Multifocal optical device with novel phase zone plate and method for making *US Patent* 4 995 714
- [85] Love G and Scott V D 2001 Electron probe microanalysis using soft X-rays—a review: Part 1. Instrumentation, spectrum processing and detection sensitivity *J. Microsci.* **201** 1–32
- [86] Lerner J M and Laude J P 1983 New vistas for diffraction gratings *Electro-Opt.* 77–82
- [87] Kwon O K, Kim K H, Sim E D, Kim J H and Oh K R 2005 Monolithically integrated multiwavelength grating cavity laser *IEEE Photon. Technol. Lett.* **17** 1788–90
- [88] Kwon O K, Kim J H, Kim K H, Sim E D, Kim H S and Oh K R 2005 Monolithically integrated grating cavity tunable lasers *IEEE Photon. Technol. Lett.* **17** 1794–6
- [89] Wang W M, Gratten K T V, Palmer A W and Boyle W J O 1994 Self-mixing interference inside a single-mode diode laser for optical sensing application *IEEE J. Lightwave Technol.* **12** 1577–87
- [90] Kane D M and Shore K A 2005 *Unlocking Dynamical Diversity: Optical Feedback Effects on Semiconductor Lasers* (New York: Wiley)
- [91] Tkach R W, Kataja K J, Alajoki T, Karioja P and Howe D G 1986 Regimes of feedback effects in 1.5 μm distributed feedback lasers *IEEE J. Lightwave Technol.* **4** 1655–61
- [92] Pan M W, Shi B-P and Gray G R 1997 Semiconductor laser dynamics subject to strong optical feedback *Opt. Lett.* **22** 166–8
- [93] Jones R J, Spencer P S, Lawrence J and Kane D M *et al* 2001 Influence of external cavity length on the coherence collapse regime in laser diodes subject to optical feedback *IEE Proc. Optoelectron.* **148** 7–12
- [94] Huyet G *et al* 2004 Quantum dot semiconductor lasers with optical feedback *Phys. Status Solidi a* **201** 345–52
- [95] Hsu T-R 2004 *MEMS Packaging* (London: Inspec)
- [96] Li J, Zhang X M, Liu A Q, Lu C and Hao J Z 2005 A monolithically integrated photonic MEMS subsystem for optical network applications *Opt. Commun.* **249** 579–86
- [97] Liu A Q, Zhang X M, Cai H, Tang D Y and Lu C 2005 Miniaturized injection-locked laser using microelectromechanical systems technology *Appl. Phys. Lett.* **87** 1–3 101101